Supporting Information for:

Enhanced Cell Death Imaging Using Multivalent Zinc(II)-Bis(dipicolylamine) Fluorescent Probes

Bryan A. Smith, Shuzhang Xiao, Kara M. Harmatys, Erin L. Cole, Adam J. Plaunt, William Wolter, Mark A. Suckow, and Bradley D. Smith*

Table of Contents

1. Vesicle Titration Data S2

2. Fluorescence Microscopy of Cell Death S3

3. Spontaneous Prostate Tumor Imaging S7

4. Longitudinal In Vivo Imaging of Traumatic Brain Injury S8

5. Quantification of In Vivo Imaging of Traumatic Brain Injury S9

6. Cold Block Study in Traumatic Brain Injury Model S10

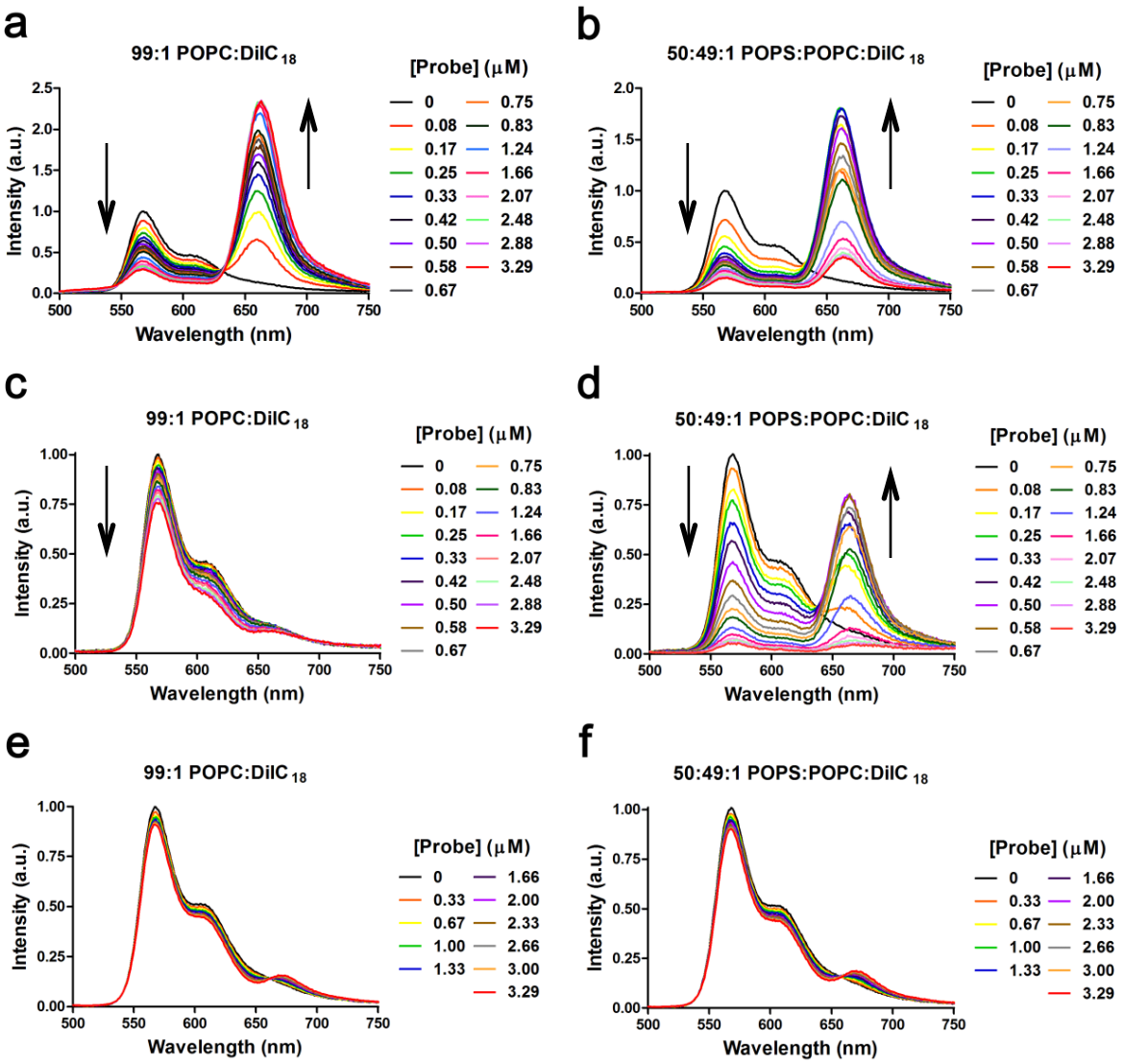

Figure S1. Normalized fluorescence spectra (ex: 480 nm) showing FRET induced by incremental addition of squaraine rotaxane probe (em: 670 nm) as energy acceptor to vesicles containing 1 mol % of the energy donor $DiIC_{18}$ (em: 570 nm) and either 99 % POPC, or 49:50 % POPC:POPS mixture (10 μM total phospholipid) in HEPES buffer, pH 7.4. (a, b) Bis-Zn_2BDPA-SR, (c, d) Tetra-Zn_2BDPA-SR, (e, f) Tracer-653. The change in $DiIC_{18}$ emission intensity at 570 nm is plotted in article Figure 2. Note for the experiment in panel (d); vesicle precipitation occurred once the Tetra-Zn_2BDPA-SR concentration was higher than 0.5 μM as reflected by the incremental decrease of its emission intensity at 670 nm.

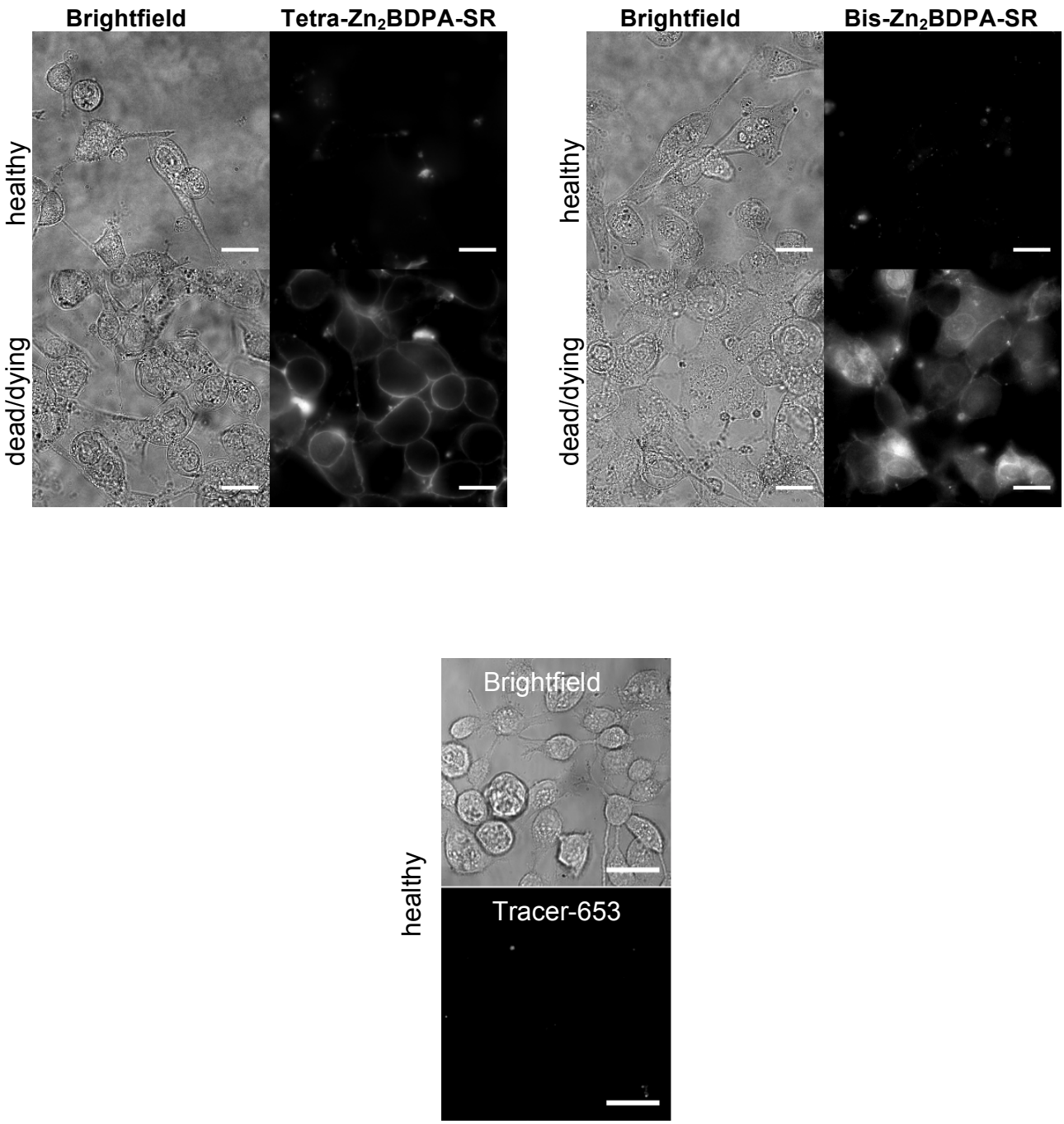

Figure S2. Brightfield and deep-red fluorescence micrographs of healthy MDA-MB-231 cells or dead/dying cells due to treatment with etoposide (15 μM) for 11 h. The cells were imaged after incubation with 10 μM of probe (Tetra-Zn_2BDPA-SR, Bisa-Zn_2BDPA-SR, or Tracer-653) for 30 min at 37 °C, followed by washing with HEPES buffer. Scale bar = 30 μm. These images expand the data presented in article Figure 3.

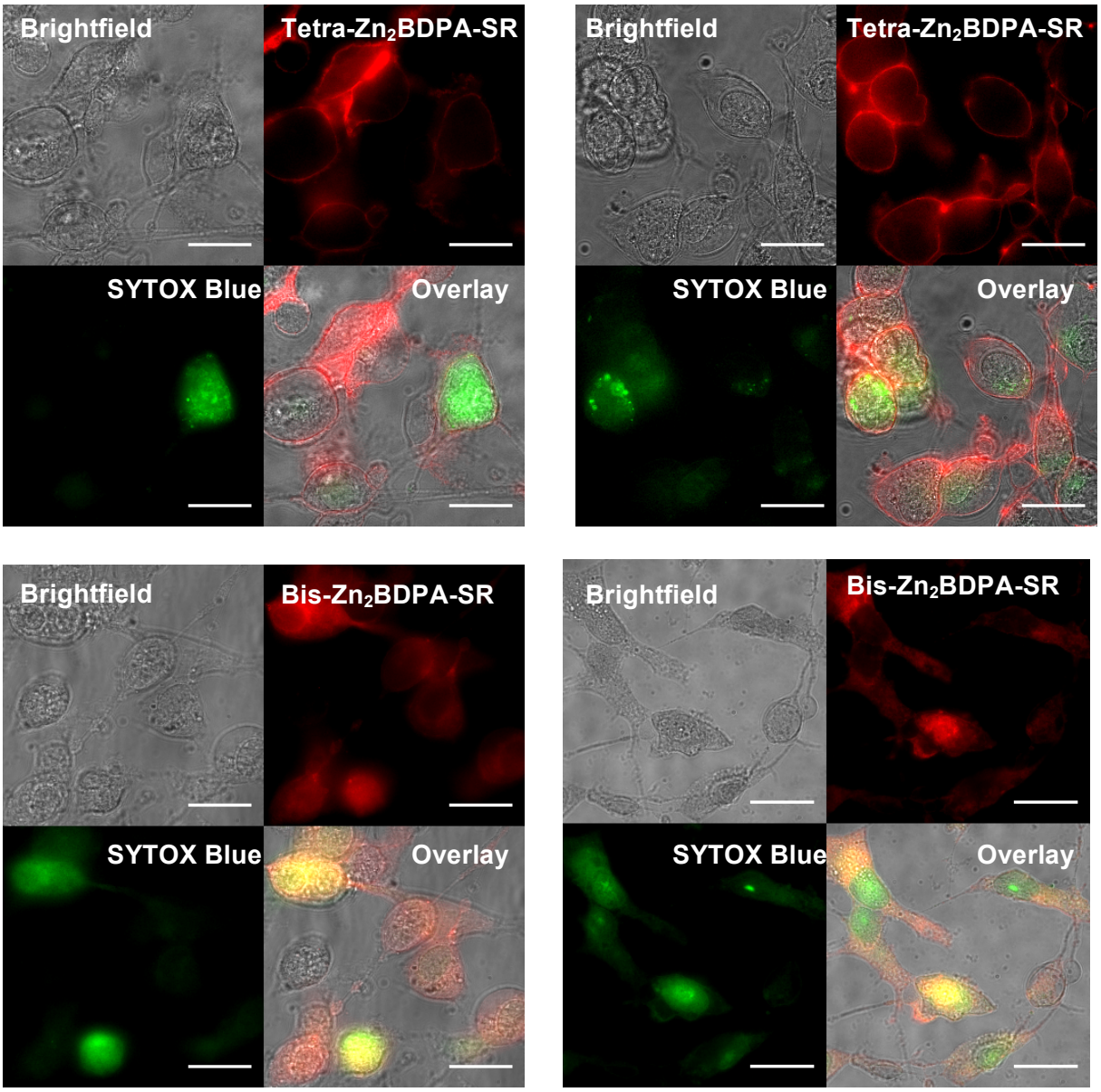

Figure S3 Expansion of the data in article Figure 4. The four panels of brightfield and fluorescence micrographs show dead/dying MDA-MB-231 cells after incubation with nucleic acid stain SYTOX Blue (5 μM) and either Tetra-Zn_2BDPA-SR or Bis-Zn_2BDPA-SR (10 μM). In each case, the cells were initially treated with etoposide (15 μM) for 11 hr, incubated with the probes for 30 min at 37 °C, then washed with HEPES buffer. Scale bar = 30 μm. Unstained cells are designated healthy, cells stained red are apoptotic, and cells stained red and green are necrotic.

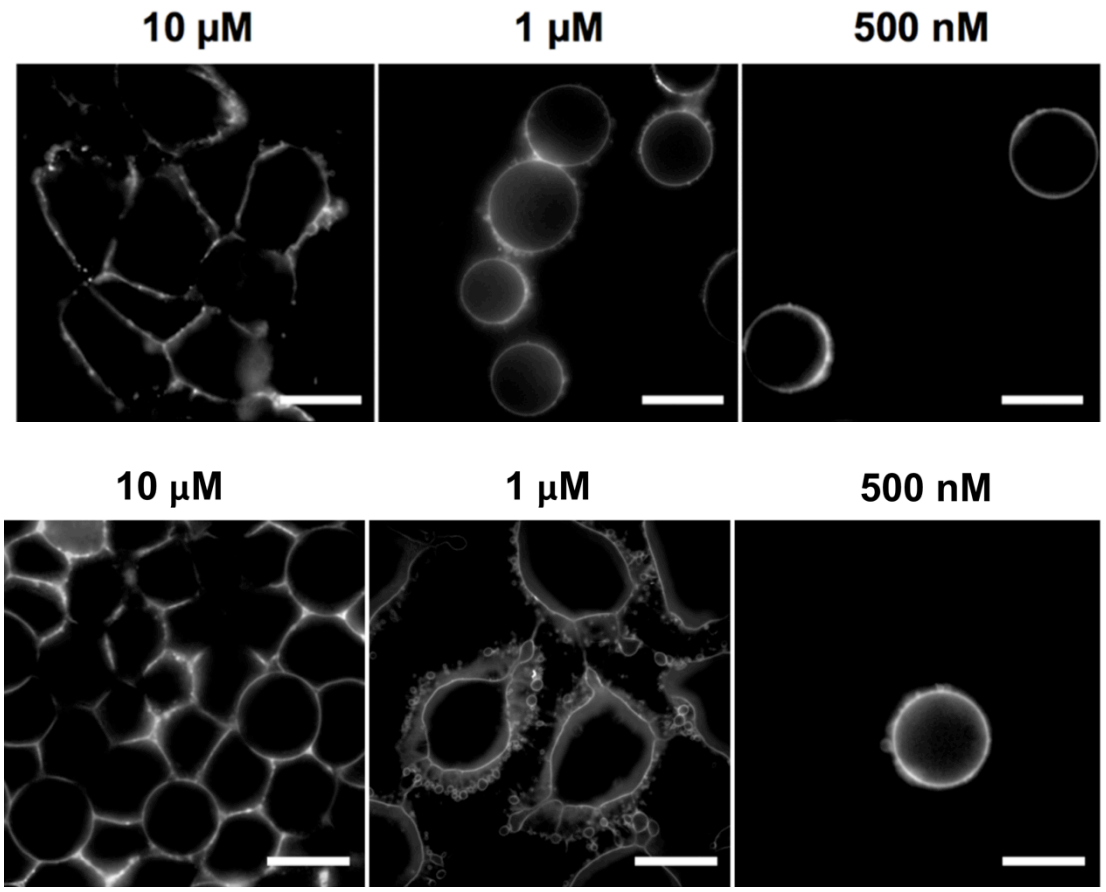

Figure S4. Deep-red fluorescence micrographs of dead and dying MDA-MB-231 cells (*top row*), or A549 cells (*bottom row*). In each case, the cells were treated with etoposide (15 μM) for 11 hr, incubated with the indicated concentration of Tetra-Zn_2BDPA-SR for 30 min at 37 °C, then washed with HEPES buffer. Scale bar = 30 μm.

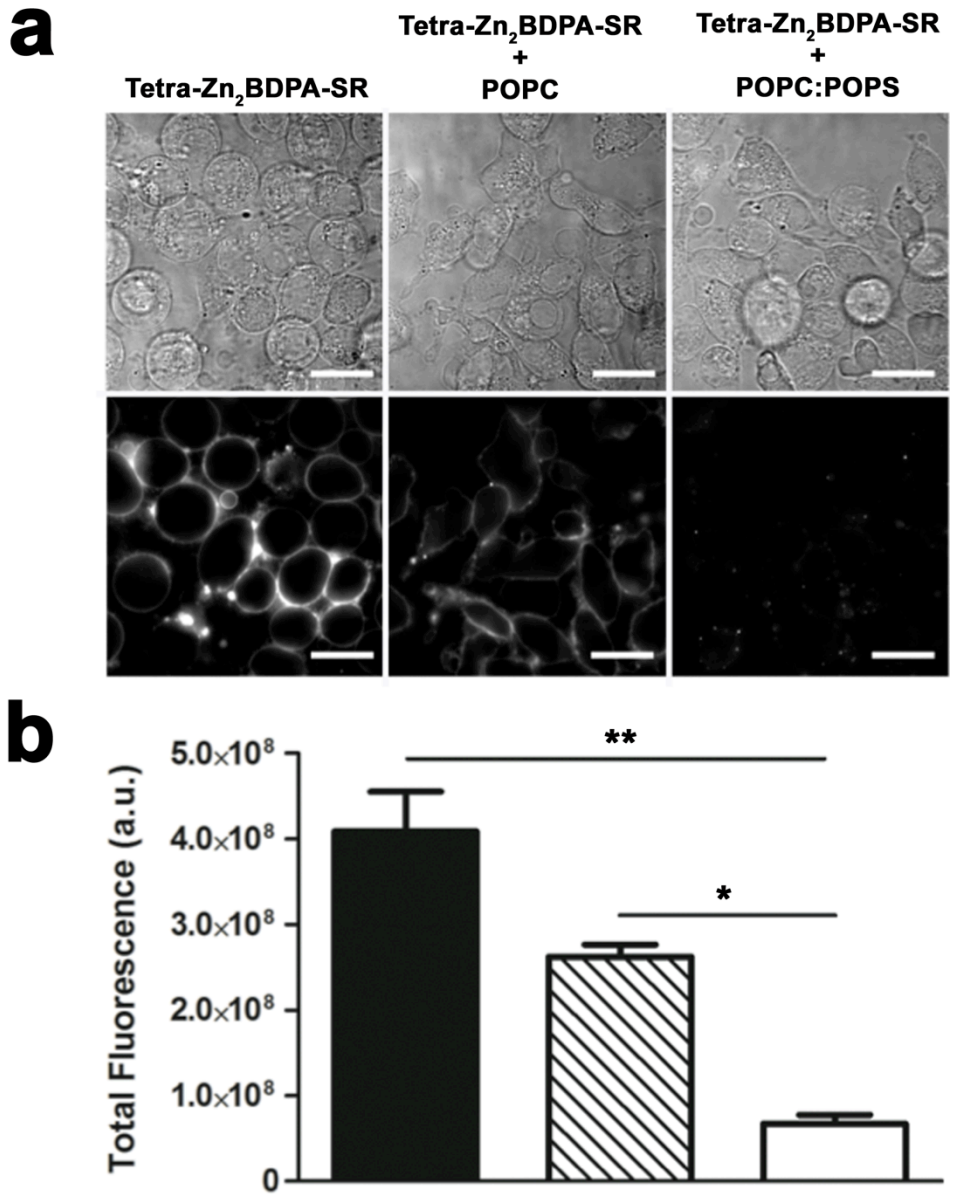

Figure S5. Cold block of Tetra-Zn_2BDPA-SR binding to dead/dying MDA-MB-231 cells using POPC and POPC:POPS (50:50) vesicles. Fluorescence microscopy of etoposide-treated MDA-MB-231 cells stained with either Tetra-Zn_2BDPA-SR alone (1 μM), Tetra-Zn_2BDPA-SR with POPC vesicles, or Tetra-Zn_2BDPA-SR with POPC:POPS (1:1) vesicles (**a**). The vesicle phospholipid concentration was 100-fold more than the concentration of Tetra-Zn_2BDPA-SR. Scale bar = 30 μm. Quantitative comparison of total fluorescence intensity for Tetra-Zn_2BDPA-SR (black bar), Bis-Zn_2BDPA-SR (dashed bar), and Tracer-653 (white bar) (**b**). The total fluorescence was measured from 6 random fields of view. * $P < 0.0002$, ** $P < 0.002$.

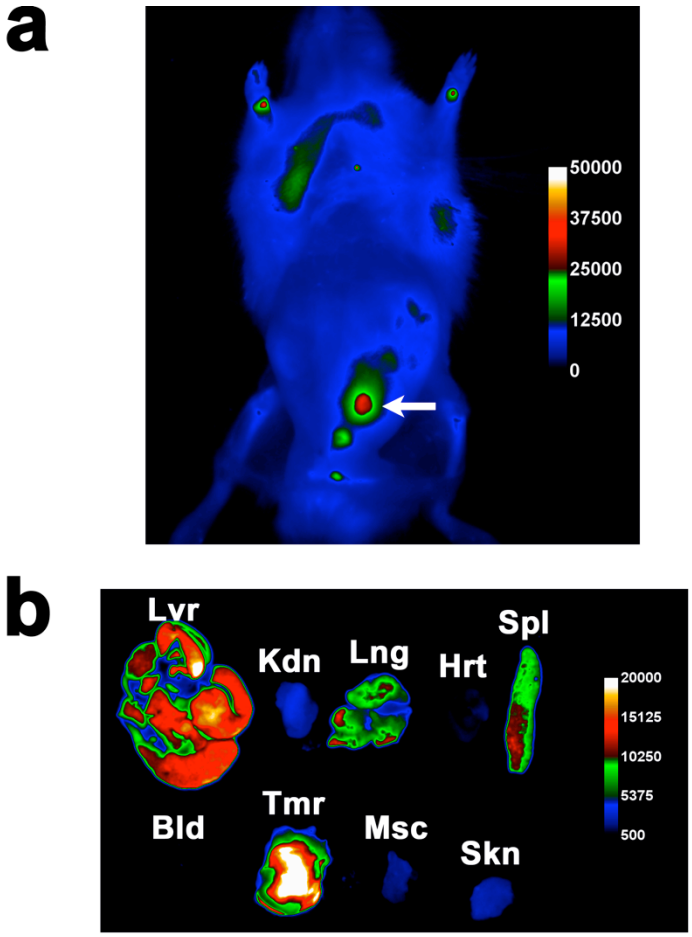

Figure S6. Representative fluorescence image of Tetra-Zn_2BDPA-SR localization to a spontaneous prostate tumor in a Lobund-Wistar rat. Image was acquired after sacrificed at 24 h post-probe injection and the skin from the lower half of the animal was removed to facilitate semi-quantitative imaging. The arrow denotes the location of the tumor (**a**). Representative ex vivo fluorescence image of Tetra-Zn_2BDPA-SR accumulation in excised rat tissues (**b**). N = 3.

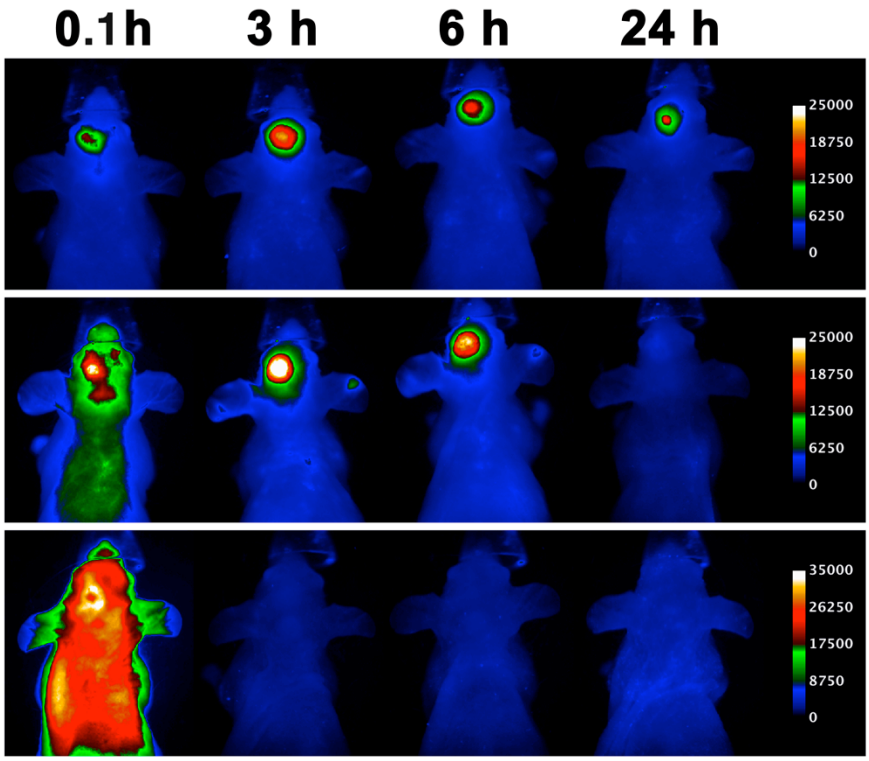

Figure S7. Representative in vivo fluorescence montages of Tetra-Zn_2BDPA-SR (top row), Bis-Zn_2BDPA-SR (middle row), and Tracer-653 (bottom row) accumulation in a traumatic brain injury mouse model. Whole-body mages of living mice were acquired at the indicated time points after probe injection. N = 4.

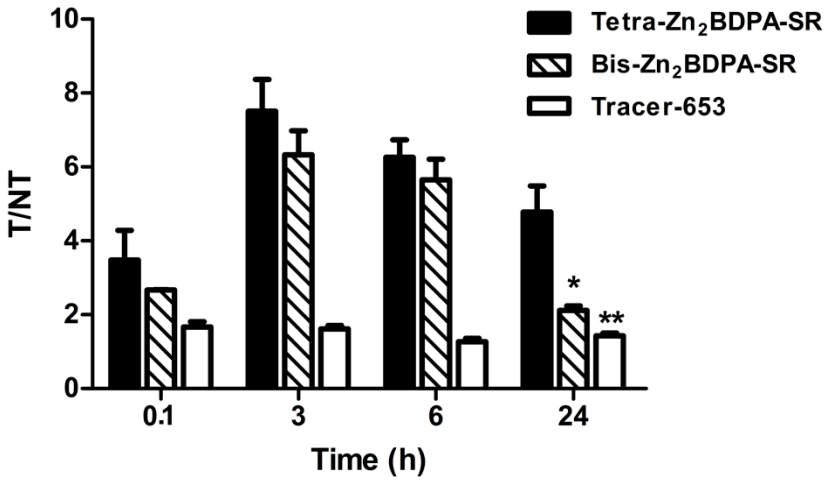

Figure S8. T/NT ratios for the in vivo fluorescence images in Figure S7. Region of interest analysis used the cryoinjury target site as T and lower back of the animal as NT. Errors bars represent the standard error of the mean. * $P < 0.03$, **$P < 0.003$. N = 5.

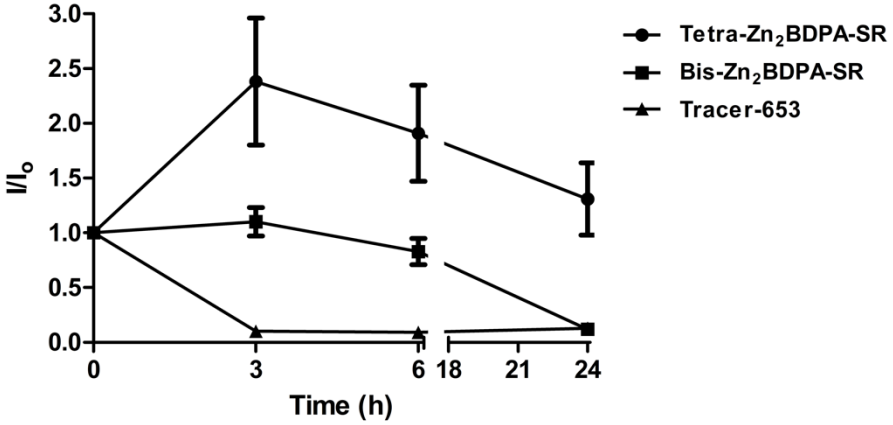

Figure S9. Normalized change in the mean pixel intensity at the site of cryoinjury for in vivo fluorescence images in Figure S7. Error bars represent the standard error of the mean. N = 5.

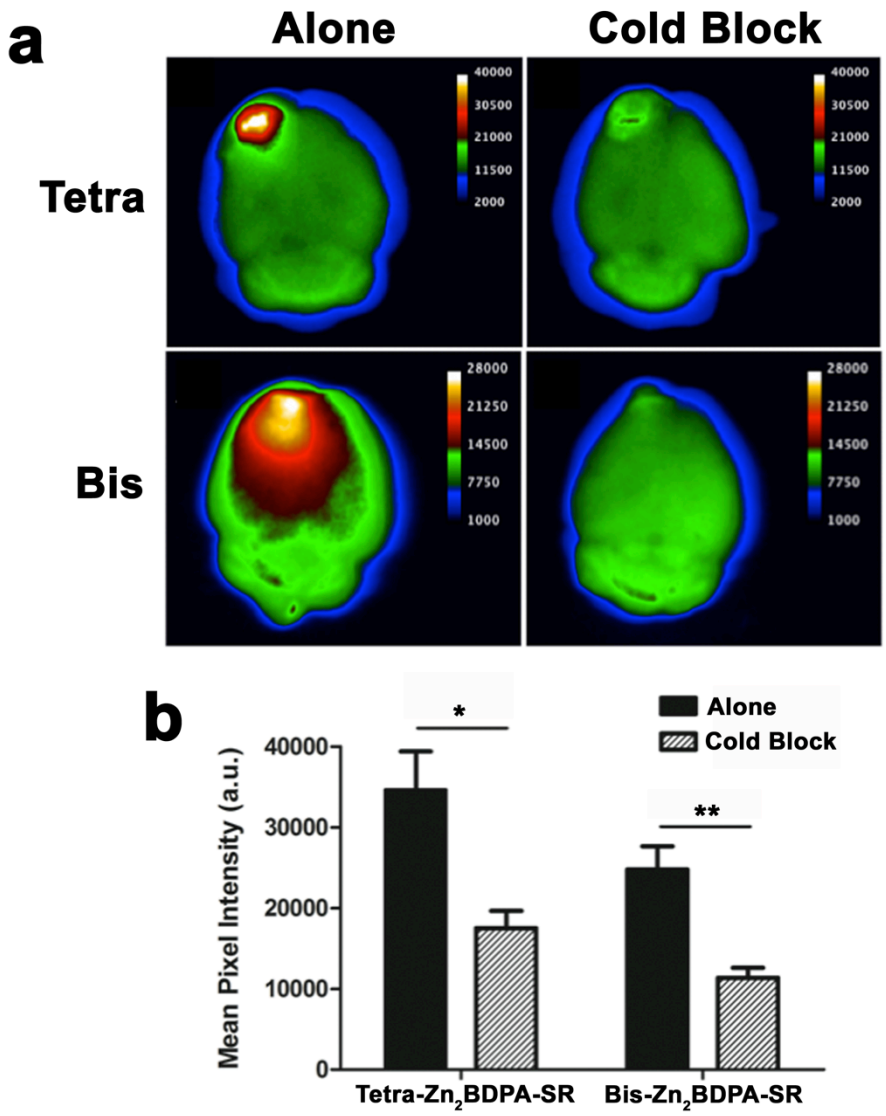

Figure S10. Cold block of Tetra-Zn_2BDPA-SR and Bis-Zn_2BDPA-SR accumulation in cryoinjured mouse brains. Representative ex vivo fluorescence images of cryoinjured brains taken from mice dosed first with vehicle control (Alone) or 15-fold molar excess of non-fluorescent Zn_2BDPA (Cold Block), then injected intravenously with Tetra-Zn_2BDPA-SR or Bis-Zn_2BDPA-SR fluorescent probe and finally sacrificed 24 h post-probe injection (**a**). Mean pixel intensities for the cryoinjury site within each ex vivo brain image, in the presence and absence of the cold block (**b**). * $P < 0.02$, ** $P < 0.005$. $N = 4$.